

Diffusion-limited reactions on a two-dimensional lattice with binary disorder

Andrea Wolff,^{*} Ingo Lohmar,[†] and Joachim Krug[‡]

Institute for Theoretical Physics, University of Cologne, Zùlpicher Strasse 77, 50937 Köln, Germany

Yecheil Frank[§] and Ofer Biham[¶]

Racah Institute of Physics, The Hebrew University, Jerusalem 91904, Israel

(Dated: September 2, 2018)

Reaction-diffusion systems where transition rates exhibit quenched disorder are common in physical and chemical systems. We study pair reactions on a periodic two-dimensional lattice, including continuous deposition and spontaneous desorption of particles. Hopping and desorption are taken to be thermally activated processes. The activation energies are drawn from a binary distribution of well depths, corresponding to ‘shallow’ and ‘deep’ sites. This is the simplest non-trivial distribution, which we use to examine and explain fundamental features of the system. We simulate the system using kinetic Monte Carlo methods and provide a thorough understanding of our findings. We show that the combination of shallow and deep sites broadens the temperature window in which the reaction is efficient, compared to either homogeneous system. We also examine the role of spatial correlations, including systems where one type of site is arranged in a cluster or a sublattice. Finally, we show that a simple rate equation model reproduces simulation results with very good accuracy.

PACS numbers: 98.38.Bn, 68.43.-h, 98.38.Cp

I. INTRODUCTION

Reaction-diffusion systems are successful models to describe a large variety of phenomena in physics, chemistry, and biology [1, 2]. They may involve one or more reactant species that diffuse and react with each other on a surface or in the bulk. In particular, surfaces often catalyze chemical reactions between adsorbed atoms and molecules. The densities of the adsorbed chemical species and their reaction rates depend on parameters of the surface and on the temperature. Microscopically, one can describe the diffusion of particles on the surface as a random walk between adsorption sites. In homogeneous systems all the adsorption sites are identical. However, most systems are heterogeneous, involving different types of adsorption sites with a broad distribution of binding energies.

The present study is motivated by a specific example of an important surface process, namely the formation of molecular hydrogen on dust grains in the interstellar medium [3–8]. Hydrogen atoms impinge from the gas phase onto a grain, and diffuse on its surface. They may either desorb thermally from the surface, or encounter each other and form a molecule. This defines a reaction-diffusion system in a spatially confined region. In this article we are concerned with steady-state systems, when the hydrogen *recombination efficiency* is defined as the fraction of impinging particles that end up (and eventually desorb) in molecular form. This efficiency plays an important role in the evolution of interstellar clouds. Typically, there is a narrow window of temperatures in which recombination is efficient. At lower temperatures, the atoms are not

sufficiently mobile to react, whereas at higher temperatures they desorb too quickly.

Assuming that all rates are spatially homogeneous, the system is well understood analytically. A zero-dimensional master equation for the particle number distribution [9, 10], together with a proper definition and calculation of the reaction rate coefficient in terms of a first-passage problem [11, 12], suffices to accurately describe the many-particle system [13]. It is very important, however, to consider disorder in the local rates of hopping and desorption of the particles. As we alluded to earlier, this is not only of theoretical interest. In fact, in the astrophysical context, the disordered case is much more realistic, and it is long known that disorder potentially enhances the efficiency dramatically [5]. However, the combination of a confined two-dimensional region, rate disorder and the many-particle reaction-diffusion dynamics makes this problem notoriously hard to tackle analytically. Kinetic Monte Carlo (KMC) methods can be used to simulate such systems [e.g. 14, 15], and algorithms are still subject to improvement [16, which also compares related approaches]. They remain computationally expensive, however, and a *systematic* understanding of the effects of disorder is still missing.

Here we start such an analysis for the simplest form of rate disorder, where each lattice position corresponds to either a standard (‘shallow’) site, or to a strong-binding (‘deep’) site, with enhanced binding energy. While we strive to keep this a theoretical self-contained work, our models and questions are motivated by applications and should easily translate to practice. This is one reason why we have chosen thermally activated rates throughout, and present most results in terms of temperature, and on scales relevant to the astrophysical problem just described. In the latter context, our work is relevant to systems combining physisorption (shallow sites) and chemisorption (deep sites) [17], aside from features particular to specific material systems. Using such a discrete distribution turns out to be conceptually different from the case of continuous distributions of binding strength [14], in which well

^{*}Electronic address: awolff@thp.uni-koeln.de

[†]Electronic address: il@thp.uni-koeln.de; now at: Racah Institute of Physics, The Hebrew University, Jerusalem 91904, Israel

[‡]Electronic address: krug@thp.uni-koeln.de

[§]Electronic address: yecheil.frank@mail.huji.ac.il

[¶]Electronic address: biham@phys.huji.ac.il

depths drawn from tails of the distribution may significantly affect the temperature window of high efficiency.

Our goal in this paper is to provide a thorough understanding of all relevant mechanisms of the described reaction-diffusion system. Most importantly, if we start from homogeneous systems of either standard or deep sites, their temperature windows of high efficiency will typically be separated by a gap. It is a natural question whether a mixture of the two types of sites still exhibits two separated peaks, or whether (and under what conditions) the efficiency is high for in-between temperatures.

Our findings are relevant for other systems as diverse as catalysts [18], exciton trapping in photosynthesis [19], exciton transport in semiconducting nanosystems [20], and diffusion-limited reactions on biomembranes [21]. The generalization of our results to these and other related contexts should be straightforward.

The paper is organized as follows. In Sec. II we define the system and our notation. The following Sec. III provides a qualitative picture which identifies three temperature regimes and describes the relevant processes in each. In Sec. IV we give a systematic account of extensive KMC simulations and discuss the observed behavior in detail. This includes the study of spatial correlations in the quenched disorder. Section V presents a simple yet accurate rate equation model, and we explain the difference to the homogeneous case. We derive an expression for the efficiency in the most interesting regime. Finally, we present our conclusions in Sec. VI.

II. MODEL AND DEFINITIONS

We consider a system of a single particle species on a two-dimensional square lattice of S sites with periodic boundary conditions. Each lattice site is characterized by a binding energy, which can take one of two values — we call this a *binary lattice*. The number of sites of either type is denoted by S_i ($i = 1, 2$), and $S = S_1 + S_2$. Particles impinge onto the lattice at a homogeneous rate f per site. If a site is already occupied, the impinging particle is rejected. In the context of surface chemistry this is known as Langmuir-Hinshelwood (LH) rejection [22].

Particles explore the lattice by hopping to neighboring sites with an (undirected) rate a , and they can desorb from a site with rate W . Both rates depend on the binding energy at the particle position. If two particles meet on one site, they form a dimer and leave the system immediately. The key quantity of such a system is the *efficiency* η , defined as the ratio between the number of particles that react and the total number of impinging particles, when the system is in a steady state.

In view of possible applications, we choose rates to be thermally activated by a system temperature T . The activation energy for desorption is denoted E_{W_i} , which we identify with the binding energy at the particle position. Similarly, hopping from a type- i site has an activation energy E_{a_i} . All rates share the attempt frequency ν , so that, e.g., $W_i = \nu \exp(-E_{W_i}/T)$ — here and in the following energies are measured in temperature units. We want to ensure *detailed balance*. The simplest

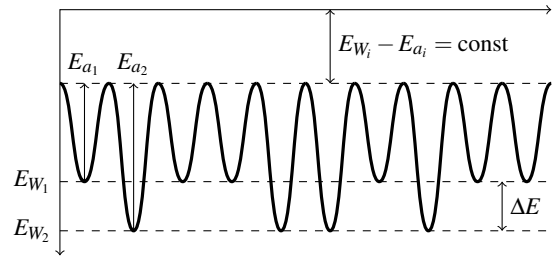


FIG. 1: One-dimensional cut through the energy landscape of our model.

way to achieve this is by choosing $W_1/a_1 = W_2/a_2$, or equivalently, $E_{W_1} - E_{a_1} = E_{W_2} - E_{a_2}$, and we will employ this choice throughout. The number of sites visited by a single particle before desorption becomes then independent of disorder.

To establish a connection to surface chemistry problems, we think of type-1 sites as standard or ‘shallow’ adsorption sites, and of type-2 sites as strong-binding or ‘deep’ sites, with $E_{W_2} > E_{W_1}$. A one-dimensional cut through such an energy landscape is sketched in Fig. 1.

III. QUALITATIVE DISCUSSION

A. Homogeneous systems

For a homogeneous lattice, the dependence of the efficiency on the temperature, $\eta(T)$, is known [9, 10]. At low temperatures the particles are nearly immobile, thus they do not meet other particles. Therefore, the lattice is highly occupied, incoming particles are mostly rejected, and the efficiency is low. For higher temperatures, hopping processes are activated and the particles begin to explore the lattice. This leads to more frequent encounters, so the efficiency rises. When the temperature is increased even further, the particles tend to desorb before encountering each other, the lattice coverage becomes small, and the efficiency decreases.

For the homogeneous system, the corresponding temperature bounds have been obtained using rate equations [10]:

$$T^{\text{up}} = \frac{2E_W - E_a}{\ln(\nu/f)} \quad (1)$$

is the temperature above which the kinetics becomes second- (instead of first-) order, whence desorption ends the typical particle residence and the efficiency is low, and

$$T^{\text{low}} = \frac{E_a}{\ln(\nu/f)} \quad (2)$$

is the temperature below which particles arrive faster than they hop, leading to dominant LH rejection and low efficiency. The average of these two bounds reads

$$T^{\text{max}} = \frac{E_W}{\ln(\nu/f)} \quad (3)$$

and corresponds to the temperature of maximum efficiency.

If the binding energy E_W is increased, the efficiency maximum is shifted towards higher temperatures, and the shift is directly proportional to the change in binding energy. For a binding energy difference $\Delta E = E_{W_2} - E_{W_1}$ of two (otherwise equal) lattices of either type-1 or type-2 sites, the relation between the temperatures of maximal efficiency is given by

$$T_2^{\max} = T_1^{\max} \cdot \left(1 + \frac{\Delta E}{E_{W_1}}\right), \quad (4)$$

whereas the peak width $T_i^{\text{up}} - T_i^{\text{low}}$ is the same.

B. Binary systems

Now we consider the binary lattice introduced in Sec. II, with binding energies E_{W_1} and E_{W_2} . To each site, we randomly assign a binding energy. There is a typical length for a particle to find a strong-binding site. This length obviously shortens when there are more and more of these sites on the lattice. At low temperatures around the efficiency maximum of the type-1 sites, particles can only diffuse on and desorb from these shallow sites, while particles landing on or hopping onto strong-binding sites cannot leave by hopping or desorption, since the binding energy is too high. Recombinations either take place on the shallow sites, or by hopping to an occupied neighboring strong-binding site. For very high temperatures around the efficiency maximum of the deep wells, the particles diffuse on, desorb from and recombine on those, while on the shallow sites, they desorb too quickly to allow any other processes. But in the intermediate temperature regime — right of the shallow peak, left of the strong-binding peak — something different happens. Here, the temperature is too low for dynamics on deep wells, so particles encountering a deep well are stuck. On the other hand, particles on shallow sites tend to desorb rather quickly, and thus do not recombine on such sites. But if they find a deep well before desorbing, they are trapped until another adatom shares their fate and they recombine.

The simple random walk with traps has been studied extensively [e.g. 19, 23]. To leading order, the average number of steps a random walker performs before trapping is given by

$$\langle n \rangle \approx \frac{1}{\pi} \frac{1}{S_2} S \ln S, \quad (5)$$

where S_2 is the number of deep wells and S is the total number of sites on the lattice. This leads to a trapping length

$$\ell_{\text{trap}} = \sqrt{\langle n \rangle}. \quad (6)$$

On the other hand, the typical radius of the area a walker explores on standard sites before desorption is the random walk length [12]

$$\ell_{\text{rw}} = \sqrt{\frac{a_1}{W_1}}. \quad (7)$$

Trapping now competes with desorption from shallow sites; the former only depends on the number of traps S_2 , while the

latter is a function of temperature. As long as the random walk length ℓ_{rw} is larger than the trapping length ℓ_{trap} , the particles are — on average — trapped before they can leave the lattice. For a given number of traps S_2 this implies a high efficiency approximately up to the temperature T^{eq} where both lengths become equal. If this temperature lies above the intermediate temperature range where both pure systems have poor efficiency, we can expect a high efficiency throughout, hence a full ‘bridging’ of the gap. Since the efficiency is high over this whole temperature range then, we call this an efficiency *plateau*. We will calculate the value of the efficiency on such a plateau in a rate equation model in Sec. VC.

Summing up, we can divide the temperature axis into three regions. The lowest temperatures where only particles on shallow sites are mobile, the intermediate regime where the particles behave like random walkers on a lattice with traps, and the high temperatures where particles become mobile on strong-binding sites. We now check this qualitative picture with KMC simulations.

IV. KINETIC MONTE CARLO SIMULATIONS

A. Setup

In order to test our predictions, we carried out extensive kinetic Monte Carlo simulations. The standard algorithm proceeds as follows [cf. 24, for a review]. We keep track of the full microscopic dynamics of continuous-time random walkers [25] with standard exponential waiting time distributions. In each simulation step, the current system configuration determines the list of possible elementary processes and their rates. By comparing a random number with the normalized partial sums of these rates we find the process to execute next. The simulation time is then advanced according to the total sum of rates and the configuration is updated.

For a given realization, we wait for the system to reach the steady state before we measure the efficiency over 10^6 impingements. We use a square lattice of $S = 100 \times 100$ sites. We choose the other model parameters inspired by an exemplary system in the astrophysical application, to show the relevance of our work in this field, and since the corresponding system is known to exhibit interesting kinetic regimes. The flux of hydrogen atoms per unit surface area depends on gas density and temperature. The flux per surface site is given by the ratio between the flux per unit area and the density of adsorption sites, hence it depends on the surface morphology. More precisely, the flux per site is given by $f = \rho v / (4s)$, where ρ is the density of hydrogen atoms in the gas phase, v is their average thermal velocity and s is the density of adsorption sites on the surface. To obtain typical values we use $\rho = 10 \text{ cm}^{-3}$, $v = 1.45 \times 10^5 \text{ cm/s}$ (which corresponds to a gas temperature of 100 K) and $s = 5 \times 10^{13} \text{ cm}^{-2}$ which is the measured density of adsorption sites on the amorphous carbon sample studied in Ref. 26. This results in a flux per site of $f = 7.3 \times 10^{-9} \text{ s}^{-1}$. For the attempt frequency we choose the standard value of 10^{12} s^{-1} which is commonly used throughout surface science. With each site we associate either the

standard binding energy $E_{W_1} = 658$ K, as found for hydrogen atoms on amorphous carbon [27], or an enhanced energy $E_{W_2} = E_{W_1} + \Delta E$ with $\Delta E = 250, 750$ or 1500 K. The activation energy for hopping reads $E_{a_1} = 511$ K or $E_{a_2} = E_{a_1} + \Delta E$, respectively.

In each case, we determine the efficiency as a function of the temperature T , as well as of the relative frequency of strong-binding sites S_2/S . We do this for up to four different ways of distributing the binding strengths. For dynamics with nearest-neighbor hopping of the particles, we either *randomly assign* to each site a binding energy with probabilities p_1 and $p_2 = 1 - p_1$, respectively, or we arrange the strong-binding sites in a regular *sublattice*, or we concentrate all strong-binding sites in a single square *cluster*. In the case of random assignment, S_2 is then binomially distributed with parameter p_2 . To eliminate the fluctuations in S_2 , we average the efficiency over 20 realizations. In the following discussion, we can therefore identify S_i/S with its average p_i . For comparison with the rate equation model to be introduced in Sec. V, we also implement another kind of dynamics (*‘longhop’ case*), namely hopping from any site to any other site of the lattice. This switches off any spatial correlations between the lattice sites and thus is best suited for comparison with an effective zero-dimensional model.

Binary disorder models very similar to random assignment and the clustered case have been simulated before [14]. The authors were predominantly concerned with showing that such models can exhibit efficient reaction over a broader range of temperatures than homogeneous systems. Here we extend these findings to a systematic picture for the effect of the deep-site fraction p_2 and the energy gap ΔE . More importantly, we provide detailed explanations and analytic results which explain all notable features of the simulation outcome in terms of microscopic physical processes.

B. Results

Figure 2 shows the results of our simulations. For each ΔE , we simulated systems with 1, 4, 25 and 50% of strong-binding sites. The random distribution is probably the most interesting regarding applications. Following the series of Figs. for each ΔE , we observe that the intermediate temperature regime is bridged in each case. This is in accordance with the analytic prediction of Sec. III B, since already for moderate deep-site fraction, the trapping length ℓ_{trap} is smaller than the random walk length ℓ_{rw} for all intermediate temperatures. The observation holds at least up to $\Delta E = 2500$ K (not shown), which is the largest value of ΔE that we have considered; beyond this energy scale one enters the regime of chemisorption, which is not our focus in this work. The bigger the difference of the binding energies, the more strong-binding sites are needed to form a genuine plateau, where the efficiency does not depend on the temperature. This complies with the ideas of Sec. III; when the deep-site peak is shifted to higher temperatures, T^{eq} has to increase to warrant formation of a plateau. This is achieved by increasing the deep-site fraction. The variance of the efficiency between different realizations of random land-

scapes was found to be negligible throughout. We also examined the longhop case on such landscapes, and found that the efficiency varies just as much. Since this cannot be affected by any spatial correlations, we conclude that this variation is always due to fluctuations in the number of deep sites S_2 only.

The arrangement of strong-binding sites in a sublattice performs slightly better, compared to random assignment. This is not astonishing since the sublattice optimizes the distance between the traps. In the random case, small clusters of strong-binding sites can occur, in which a single trap is less efficient. An alternative picture is that the capture zones of individual traps typically have an overlap, which is minimized in the sublattice case.

On a lattice with a single square cluster of strong-binding sites, there is no bridging effect for any energy difference or frequency of strong-binding sites. For high frequencies of either shallow or strong-binding sites, only one restricted peak emerges, while for intermediate frequencies of strong and shallow sites two nearly separated peaks appear. The efficiency does not drop to zero in the intermediate temperature regime, because an exchange between shallow and deep sites takes place along the boundary of the cluster. However, since the boundary length scales as \sqrt{S} , the fraction of boundary sites decreases with increasing S , and correspondingly the suppression of the efficiency in this regime becomes even more pronounced for larger systems. We checked this for a system of 500×500 sites (not shown). This is in contrast to the well-mixed case, where a finite fraction of sites are boundary sites (see below).

For the longhop case, we first verified that results on a sublattice and a cluster landscape coincide, ensuring the correctness of the algorithm. The efficiency for this kind of dynamics outperforms even the sublattice results for nearest-neighbor hopping. This is because in the sublattice case, there is still the necessity for a particle to actually travel to a trap instead of having a non-zero probability to reach a trap on every step. A further analysis of this model is provided in Sec. V.

In addition to our qualitative explanations, we numerically examine the dependence of the plateau efficiency value on the number of deep wells. First we note that for our choice of parameters, the efficiency value at $T_1^{\text{max}} \approx 14$ K always corresponds to the plateau value. From the results for $\Delta E = 750$ K shown in Fig. 3 we infer that the way of distributing the strong-binding sites is of crucial importance. In the case of a single square cluster of deep wells, the efficiency decreases linearly as $1 - S_2/S$, while for the random distribution the efficiency first decreases more slowly (for less than 50% of strong-binding sites) and faster to the end (more than 50%). We propose that this effect is related to the border length between shallow and deep sites, and use this connection to derive an empirical formula for the plateau efficiency. For randomly distributed deep wells, we calculate the border length L as function of S_2/S (cf. Fig. 4). We find a shallow site next to a deep site with probability $(S_2/S)(1 - S_2/S)$. Since the orientation of the pair does not matter, we gain an additional factor of 2. Furthermore we have $2S$ possibilities to place such a pair of sites on a square lattice with S sites and periodic boundary conditions. So we find the following expression for the border

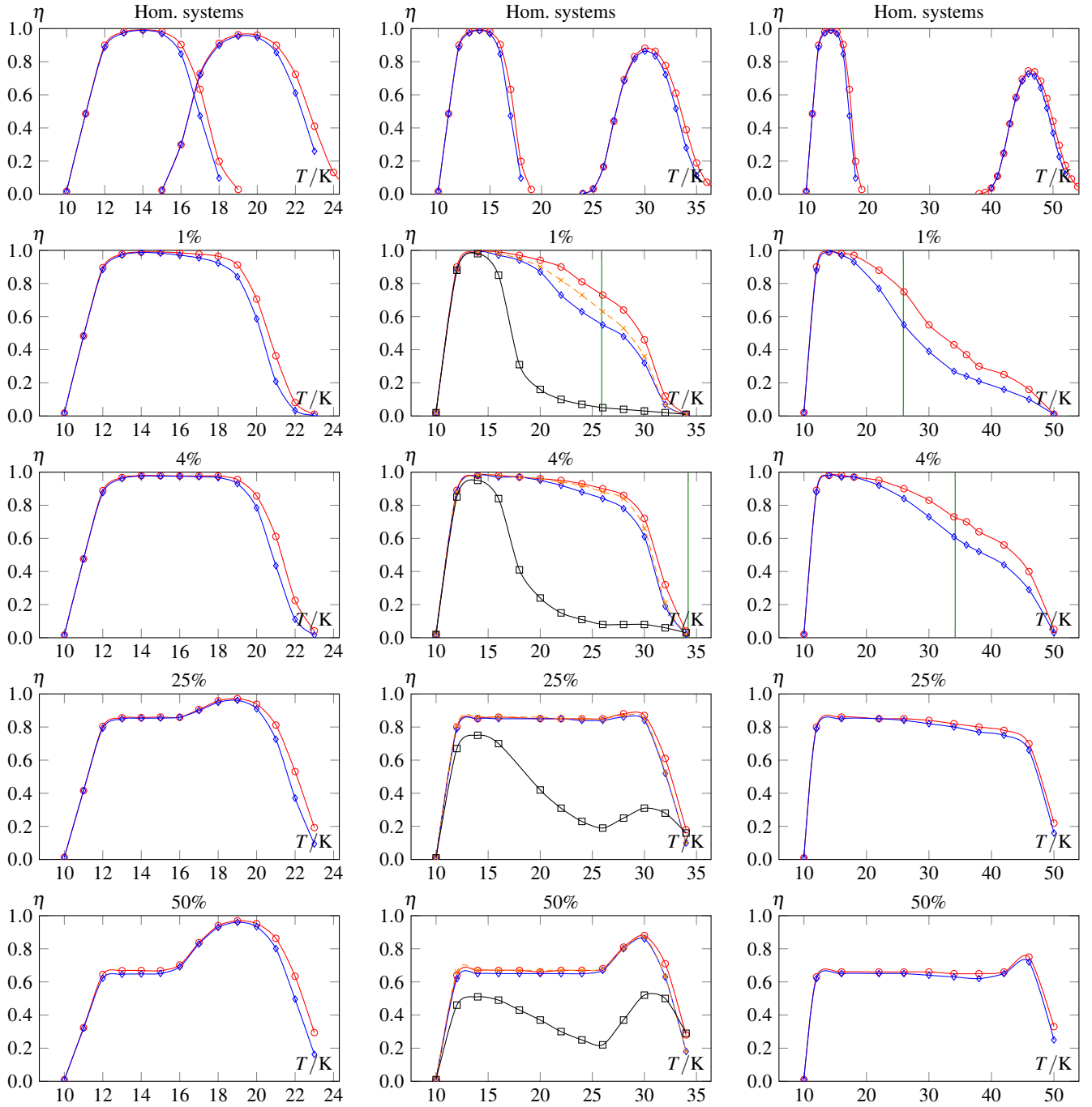


FIG. 2: (Color online) Efficiency versus temperature for various fractions of deep sites. Left column $\Delta E = 250$ K, middle $\Delta E = 750$ K, right $\Delta E = 1500$ K. Randomly assigned energies (blue line, diamonds), longhop dynamics (red line, circles). Only for $\Delta E = 750$ K: sublattice (orange dashed line, crosses), and cluster (black line, squares). Vertical green line at T^{eq} . The first row shows the results for homogeneous systems of only standard or only deep sites, respectively.

length between shallow and deep sites

$$L = 4S \cdot \frac{S_2}{S} \left(1 - \frac{S_2}{S} \right). \quad (8)$$

Fitting the efficiency difference $\Delta\eta = \eta_{\text{random}} - \eta_{\text{cluster}}$ to a

multiple of this border length yields

$$\Delta\eta = C \cdot L, \quad (9)$$

with $C = (1.487 \pm 0.019) \times 10^{-5}$ or

$$\eta_{\text{random}} \approx \left(1 - \frac{S_2}{S} \right) \cdot \left(1 + (0.595 \pm 0.008) \frac{S_2}{S} \right) \quad (10)$$

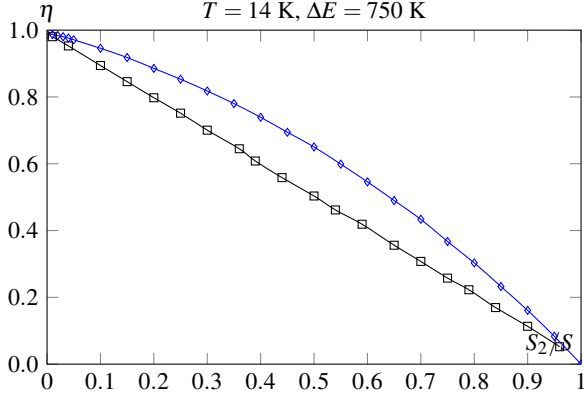


FIG. 3: (Color online) Efficiency as function of the deep-site fraction for $T = 14$ K and $\Delta E = 750$ K, for clustered deep sites (black, squares, η_{cluster}) and randomly assigned energies (blue, diamonds, η_{random}).

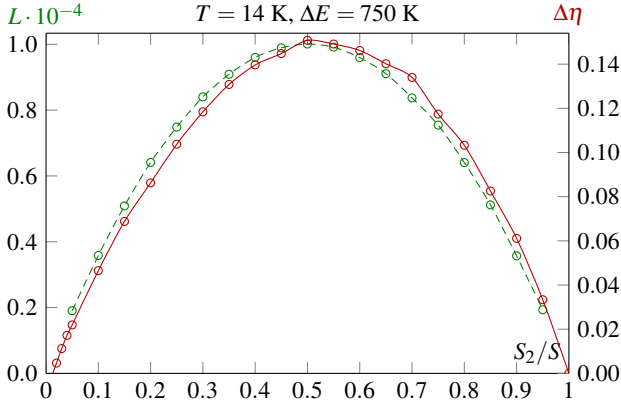


FIG. 4: (Color online) Border length L (green dashed line, left axis) and efficiency difference $\Delta\eta$ (dark red, right axis), as function of deep-site fraction, for $T = 14$ K and $\Delta E = 750$ K. Vertical axis scaling taken from data fit.

for the empirical plateau efficiency value. The quality of the fit $\Delta\eta \propto L$ for KMC results underlines the role of the border length, and this corroborates our picture that the dominant reaction process on the plateau is by hopping from standard to deep sites. Further insight into the origin of Eq. (10) will be provided below in Sec. VC.

V. RATE EQUATION MODEL

Rate equations have been used previously to study reactions on finite surfaces with different types of sites. Using surfaces with varying roughness, where binding energies at a site are given by a vertical bond strength plus an additional lateral bond strength per in-layer neighbor of the landscape, KMC simulations were performed [15]. A rate equation model was then used to check that such a rough landscape model is consistent with surfaces deemed astrophysically relevant and examined in the laboratory. To this end, the rate equations with

standard energy parameters were time-integrated to predict the results of TPD experiments.

Here we apply a rate equation model to quantitatively reproduce our KMC findings as well as to further our qualitative understanding of the system's behavior. From the definition of Sec. II we derive a set of rate equations for the total number N_i of particles on sites of type i . Terms for desorption and influx are easily written down, whereas the reaction terms are more subtle, partly since in general, the reaction is not an elementary process with given rate. For the time being, we denote the appropriate rate coefficients as A_i , and refer to Sec. VA for details. The rate equations then take the form [15, 28]

$$\begin{aligned} \frac{\dot{N}_1}{t} &= f(S_1 - N_1) - W_1 N_1 - A_1 N_1 (S_2 - N_2) - A_1 N_1 N_2 \\ &\quad - 2A_1 N_1^2 + A_2 N_2 (S_1 - N_1) - A_2 N_1 N_2, \\ \frac{\dot{N}_2}{t} &= f(S_2 - N_2) - W_2 N_2 - A_2 N_2 (S_1 - N_1) - A_2 N_1 N_2 \\ &\quad - 2A_2 N_2^2 + A_1 N_1 (S_2 - N_2) - A_1 N_1 N_2. \end{aligned} \quad (11)$$

Here the first two contributions cater for the impingement flux with rejection and the desorption of particles. For clarity we separated the remaining terms. The next two terms describe leaving to a site of the opposite type (either to an empty or to an occupied site). Then we account for reactions inside one population due to hops between sites of the same type, removing two atoms. The remaining two contributions describe gaining a particle by a hop from the other site type, and finally, losing one particle due to the reaction with a particle coming from the other population.

It is tempting to substitute the ‘internal’ reaction term $2A_i N_i^2$ by $2A_i N_i (N_i - 1)$, since it should really depend on the number of *pairs*. This is *not* adequate: In the rate equation treatment the N_i are continuous and can drop below unity, such that the reaction term (which we are ultimately interested in) could then become negative. The assumption that the reaction rate can be written as above is at the heart of the rate equation approach (“mass action law”). Equations (11) are easily derived from the full master equation using this assumption in the forms $\langle N_i (N_i - 1) \rangle \approx N_i^2$ and $\langle N_1 N_2 \rangle \approx N_1 N_2$ (where the expectation is over the joint probability distribution $P(N_1, N_2)$ and the r.h.s. N_i 's are already the mean values as above).

The reaction terms also provide the recombination rate of the process. Adding up all terms proportional to the A_i in $\dot{N}/t = \dot{N}_1/t + \dot{N}_2/t$, mere hopping terms (not leading to a reaction) cancel. Using that the reaction consumes two particles, we obtain the rate at which particles are removed by the reaction as

$$2R = 2A_1 N_1^2 + 2A_2 N_2^2 + 2(A_1 + A_2) N_1 N_2, \quad (12)$$

which can be simplified to $2R = 2(A_1 N_1 + A_2 N_2)(N_1 + N_2)$. Relating this to the particle influx $f(S_1 + S_2) = fS$ gives the *efficiency* $\eta = 2R/(fS)$.

A. The reaction rate coefficient

The homogeneous system was treated analytically by rate equations [10, 27, 29], the master equation [9, 10], and moment equations [30, 31]. For these methods just as for stochastic or numerical methods based on these approaches, the reaction rate coefficient is a crucial quantity, typically approximated as $A \approx a/S$ [32]. We have argued elsewhere that this neglects the nature of two-dimensional diffusion (“back diffusion”) as well as the fundamental first-passage problem, the competition between a meeting (hence reaction) of particles and the prior desorption of a reactant. Hence we put some effort into a proper definition and evaluation of A [11, 12], and we claimed that these results should be applied in all mentioned frameworks, including the rate equation treatment [13].

Here, we return to the choice $A_i = a_i/S$, since the situation is different. In rate equations such as Eqs. (11), there is no way to genuinely incorporate any spatial structure. This holds true for *all* zero-dimensional approaches, e.g., the master equation as well. However, in the homogeneous systems studied before, this neglect only concerns the spatial correlations in the particle residence probability, with well-studied effects [10, 11, 33]. In the heterogeneous system with its *separated* populations, this approach additionally neglects site type correlations.

For consistency, we are then forced to assume that a particle can reach any other site by a single hop. In particular, it hops to a site of type i with probability S_i/S , and it meets a particle on an i -site with probability N_i/S . The conventional choice $A_i \approx a_i/S$ thus arises naturally if we use rate equations to describe a system with site disorder, and we adopt this choice in the following. For a system with quenched spatial structure and nearest-neighbor hops only, this description corresponds most closely to the well-mixed case.

B. Comparison with KMC simulations

The rate equations (11) are exactly solvable at steady state by finding the real positive root of a third-order polynomial. However, the results are cumbersome and less than illuminating. We therefore directly opted for a numerical solver throughout.

We find that the rate equations for the binary system reproduce the outcome of extensive KMC (longhop) simulations for a wide parameter range of practical relevance to excellent accuracy (see Fig. 5). As noted in prior work [11], however, since we present our results as functions of temperature and parameters are thermally activated, we typically have rather steep rises or declines, when even factors of two or three in the efficiency need not appear substantial. This hardly explains the overall accuracy, especially on plateaus and moderate peaks for η considerably smaller than unity.

Results on the validity of rate equations to describe the model in the homogeneous case have shown that confinement to a finite surface renders the discreteness of particles and fluctuations in the particle number important [10, 11, 33–36]. Consequently, the mean-field approach of rate equations con-

siderably overestimates the recombination efficiency in small systems. We do not see such effects for several reasons. We are interested in the behavior of the system with a substantial number of particles, when the effects of discreteness and of fluctuations in this particle number are strongly reduced. Further, the confinement of particles to a finite surface is also far less important than for the homogeneous system, because the majority of these particles is trapped in deep wells in the regimes of most interest, anyway. Finally, our system cannot be considered small, and we cannot preclude completely that differences might be more pronounced for smaller system sizes or different activation energies.

C. Plateau efficiency

A key question of this work concerns the bridging between the two efficiency peaks corresponding to homogeneous systems of one type of sites. We have found a convincing qualitative picture before in Sec. III, and we observe an efficiency plateau between the two (virtual) peaks for a wide range of conditions. What is the value of the efficiency along this plateau?

We need to further simplify our rate equation model to arrive at a simple analytic answer. Several efforts to derive this from first principles were not met with success, hence we start from some observations: Figure 5 shows that whenever a plateau emerges in the efficiency, practically all recombinations are due to hops between the two types of sites. Only for very low concentrations of deep wells and when the efficiency is close to unity, the lower temperature end of the plateau also includes a substantial contribution from recombination on standard sites. On the high-temperature end, any sizable contribution from reactions on deep sites already results in an efficiency peak atop the plateau value anyway.

For the plateau efficiency, we can therefore capture the essence of the model accounting only for reactions *between* the two populations. Type 1 denotes the standard sites, so we clearly have $A_1 \gg A_2$. We use this to neglect *all* terms proportional to A_2 , since they are small compared to their A_1 counterparts, but keep all flux and desorption terms. Our reasoning is to retain as many terms as possible, to remove those for recombination inside the N_i populations, and since we can neglect the reaction $A_2 N_1 N_2 \ll A_1 N_1 N_2$, we have to leave out the corresponding A_2 hopping term for consistency as well. This leads to the simplified steady-state equations

$$\begin{aligned} 0 &= f(S_1 - N_1) - W_1 N_1 - A_1 N_1 S_2, \\ 0 &= f(S_2 - N_2) - W_2 N_2 + A_1 N_1 S_2 - 2A_1 N_1 N_2, \end{aligned} \quad (13)$$

which yield an efficiency

$$\eta_p = \frac{2A_1 N_1 N_2}{fS} = \frac{2fA_1 S_1 S_2 (V_1 + A_1 S)}{S(V_1 + A_1 S_2)[V_2(V_1 + A_1 S_2) + 2fA_1 S_1]}, \quad (14)$$

where $V_i = W_i + f$. We could now evaluate this at a temperature right on the plateau. It will turn out, however, that we can make two more assumptions for this case.

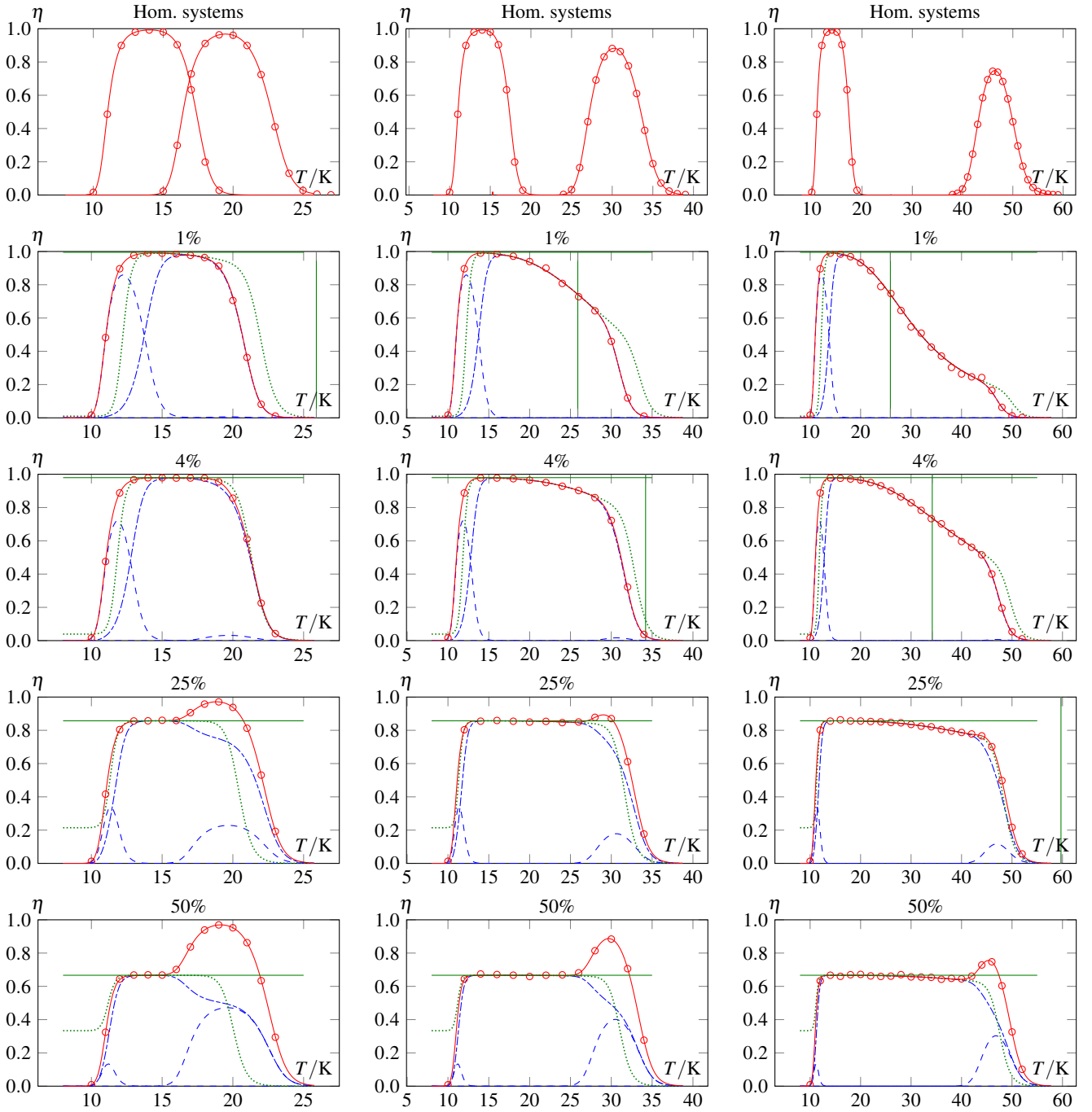


FIG. 5: (Color online) Efficiency versus temperature for various fractions of deep sites. Left column $\Delta E = 250$ K, middle $\Delta E = 750$ K, right $\Delta E = 1500$ K. Red circles: KMC longhop results (see Sec. IV). Red lines the numerical solution of rate equations with standard $A_i = a_i/S$ (solid), blue lines contributions by reaction on the 1- and 2-sites (dashed), and by switching between the types (dot-dashed). Dotted green line the results of the plateau model, and green horizontal line the simple (16). Vertical green line at T^{eq} . The first row shows the results for homogeneous systems of only standard or only deep sites, respectively.

First, we also neglect desorption from the 2-sites, so $V_2 = f$, and using $A_1 = a_1/S$, Eq. (14) reduces to

$$\eta_p = \frac{2(S_1/S)(S_2/S)(1+V_1/a_1)}{(V_1/a_1 + S_2/S)(1+V_1/a_1 + S_1/S)}. \quad (15)$$

Second, on the plateau and for a reasonable deep-site fraction

S_2/S , we have $V_1/a_1 \ll S_2/S < 1$. This yields

$$\eta_p \approx \frac{2}{S/S_1 + 1}, \quad (16)$$

which no longer depends on *any* energy scales, and which we find to be in excellent agreement with both KMC and full rate

equation results (Fig. 5): Whenever a plateau forms (i.e., if ΔE is large enough to separate the homogeneous-system peaks, and if there are enough deep wells if ΔE is fairly large), the above expression is valid.

To check the validity of these approximations, we recall from Sec. IV B that the peak temperature T_1^{\max} for standard-site parameters was found to always belong to the plateau. It is large enough not to lie on the low-temperature rise to the standard-site peak, yet minimal so as not to depend on the peak separation governed by ΔE . At $T = T_1^{\max}$, $V_1 = W_1 + f = 2f$ and $V_2 = W_2 + f = f[(f/v)^{\Delta E/E_{W_1}} + 1]$. Reasonably, $f/v \lll 1$, while the smallest interesting $\Delta E \sim E_{W_1} - E_{a_1}$, such that the ratio $\Delta E/E_{W_1}$ is not excessively smaller than unity. This justifies the approximation $V_2 \approx f$, immediately eliminating ΔE from the game, as suggested by Fig. 5. We now check the order of $V_1/a_1 = 2f/a_1 = 2(f/v)^{(E_{W_1} - E_{a_1})/E_{W_1}}$. The exponent is about 0.22 for amorphous carbon, and with the corresponding standard flux we have $V_1/a_1 \approx 6.3 \times 10^{-5}$ (cf. Sec. IV A). This is negligible compared to any interesting deep-well fraction S_2/S , which completes the argument for Eq. (16). (We checked that this holds at least equally well for standard olivine parameters [27].)

Knowing what terms can be neglected, this result is also easily derived from further simplified rate equations. We rather provide an intuitive explanation. We consider the system in the steady state, so all particles entering the system also have to leave. They enter by impingement to any site, and leave only from 2-sites, by LH rejection or by reaction with an incoming 1-particle. Consequently, particles from 1-sites arrive at a rate fS_1/S_2 at each 2-site. This implies a rate $2fS_1/S_2 \cdot N_2$ of particles to leave the system, as the reaction takes away *two* atoms. Alternatively, particles leave by LH rejection (rate-wise, this is merely a separate desorption process) at a rate $f \cdot N_2$. The efficiency is the fraction of impinging particles that react; in the steady state, this is just the rate at which particles leave due to reaction, normalized by the total rate to leave (by reaction or by LH rejection). This yields

$$\eta_p = \frac{2S_1}{2S_1 + S_2}, \quad (17)$$

which coincides with Eq. (16). We note that Eq. (17) can be rewritten as

$$\eta_p = \frac{1 - S_2/S}{1 - S_2/(2S)} \approx \left(1 - \frac{S_2}{S}\right) \left(1 + \frac{S_2}{2S}\right) \quad (18)$$

for $S_2/S \lll 1$, which is precisely of the form of the empiri-

cal relation (10). The coefficient inside the second bracket in Eq. (10) deviates from 1/2 because it was obtained through a fit over the entire range of $S_2/S \in [0, 1]$, whereas Eq. (18) is strictly valid only when S_2/S is small.

VI. CONCLUSIONS

We have studied diffusion-limited reactions of particles on a two-dimensional lattice which consists of shallow and deep sites, using KMC simulations and rate equations. In the case when the two types of sites are randomly mixed, we found that the temperature range in which the reaction is efficient dramatically broadens compared to a homogeneous system that includes only shallow or only deep sites. The rate equations are found to provide a good description of the system and are in perfect agreement with the KMC results. We have also studied a system in which the deep sites are clustered together. In this case the hopping between shallow and deep sites is suppressed. As a result, the recombination efficiency is dramatically reduced in comparison with the case in which the shallow and deep sites are randomly mixed.

We expect that the qualitative features observed for the binary distribution will hold for a broader class of models with different distributions of binding energies. The results presented in this paper are also relevant in the context of molecular hydrogen formation in the interstellar medium. More specifically, high abundances of molecular hydrogen are observed in photon-dominated regions [37]. In these regions, the grain temperatures are too high to form molecular hydrogen from weakly adsorbed hydrogen atoms. It was proposed that strong-binding sites in conjunction with the weak-binding sites enable the efficient formation of molecular hydrogen under these conditions [38, 39]. Our work provides a quantitative basis for this mechanism.

Acknowledgments

This work was supported by Deutsche Forschungsgemeinschaft within SFB/TR-12 *Symmetries and Universality in Mesoscopic Systems* and the Bonn-Cologne Graduate School of Physics and Astronomy, and by the US-Israel Binational Science Foundation. JK acknowledges the kind support and hospitality of the Hebrew University through the Lady Davis Fellowship Trust.

[1] D. ben-Avraham and S. Havlin, *Diffusion and Reactions in Fractals and Disordered Systems* (Cambridge University Press, 2000).
 [2] B. A. Grzybowski, K. J. M. Bishop, C. J. Campbell, M. Filkowski, and S. K. Smoukov, *Soft Matter* **1**, 114 (2005).
 [3] R. J. Gould and E. E. Salpeter, *Astrophys. J.* **138**, 393 (1963).
 [4] D. Hollenbach and E. E. Salpeter, *J. Chem. Phys.* **53**, 79 (1970).

[5] D. Hollenbach and E. E. Salpeter, *Astrophys. J.* **163**, 155 (1971).
 [6] D. J. Hollenbach, M. W. Werner, and E. E. Salpeter, *Astrophys. J.* **163**, 165 (1971).
 [7] R. Smoluchowski, *J. Phys. Chem.* **87**, 4229 (1983).
 [8] W. W. Duley and D. A. Williams, *Mon. Not. R. Astron. Soc.* **223**, 177 (1986).

- [9] N. J. B. Green, T. Toniazzo, M. J. Pilling, D. P. Ruffle, N. Bell, and T. W. Hartquist, *Astron. Astrophys.* **375**, 1111 (2001).
- [10] O. Biham and A. Lipshtat, *Phys. Rev. E* **66**, 056103 (2002).
- [11] I. Lohmar and J. Krug, *Mon. Not. R. Astron. Soc.* **370**, 1025 (2006).
- [12] I. Lohmar and J. Krug, *J. Stat. Phys.* **134**, 307 (2009).
- [13] I. Lohmar, J. Krug, and O. Biham, *Astron. Astrophys.* **504**, L5 (2009).
- [14] Q. Chang, H. M. Cuppen, and E. Herbst, *Astron. Astrophys.* **434**, 599 (2005).
- [15] H. M. Cuppen and E. Herbst, *Mon. Not. R. Astron. Soc.* **361**, 565 (2005).
- [16] A. G. Tsvetkov and V. I. Shematovich, *Sol. Sys. Res.* **43**, 301 (2009).
- [17] V. Mennella, *Astrophys. J. Lett.* **684**, L25 (2008).
- [18] M. T. M. Koper, J. J. Lukkien, A. P. J. Jansen, and R. A. van Santen, *J. Phys. Chem. B* **103**, 5522 (1999).
- [19] E. W. Montroll, *J. Math. Phys.* **10**, 753 (1969).
- [20] A. V. Barzykin and M. Tachiya, *J. Phys. CM* **19**, 065105 (2007).
- [21] R. Straube, M. J. Ward, and M. Falcke, *J. Stat. Phys.* **129**, 377 (2007).
- [22] I. Langmuir, *J. Am. Chem. Soc.* **40**, 1361 (1918).
- [23] J. W. Evans and R. S. Nord, *Phys. Rev. A* **32**, 2926 (1985).
- [24] A. F. Voter, in *Radiation Effects in Solids*, edited by K. E. Sickafus, E. A. Kotomin, and B. P. Uberuaga (Springer, 2007), vol. 235 of *Nato Science Series II: Mathematics, Physics And Chemistry*, URL http://www.ipam.ucla.edu/publications/matut/matut_5898_preprint.pdf.
- [25] E. W. Montroll and G. H. Weiss, *J. Math. Phys.* **6**, 167 (1965).
- [26] O. Biham, I. Furman, V. Pirronello, and G. Vidali, *Astrophys. J.* **553**, 595 (2001).
- [27] N. Katz, I. Furman, O. Biham, V. Pirronello, and G. Vidali, *Astrophys. J.* **522**, 305 (1999).
- [28] H. B. Perets, Master's thesis, The Hebrew University, Jerusalem (2004).
- [29] O. Biham, I. Furman, N. Katz, V. Pirronello, and G. Vidali, *Mon. Not. R. Astron. Soc.* **296**, 869 (1998).
- [30] A. Lipshtat and O. Biham, *Astron. Astrophys.* **400**, 585 (2003).
- [31] B. Barzel and O. Biham, *J. Chem. Phys.* **127**, 144703 (2007).
- [32] T. Stantcheva, P. Caselli, and E. Herbst, *Astron. Astrophys.* **375**, 673 (2001).
- [33] O. Biham, J. Krug, A. Lipshtat, and T. Michely, *Small* **1**, 502 (2005).
- [34] A. G. G. M. Tielens (1995), talk at a conference on interstellar chemistry in Leiden, The Netherlands.
- [35] J. Krug, *Phys. Rev. E* **67**, 065102(R) (2003).
- [36] A. Lederhendler and O. Biham, *Phys. Rev. E* **78**, 041105 (2008).
- [37] E. Habart, F. Boulanger, L. Verstraete, C. M. Walmsley, and G. P. des Forêts, *Astron. Astrophys.* **414**, 531 (2004).
- [38] S. Cazaux and A. G. G. M. Tielens, *Astrophys. J.* **604**, 222 (2004).
- [39] S. Cazaux and A. G. G. M. Tielens, *Astrophys. J. Lett.* **575**, L29 (2002).